

No-Reference Video Quality Assessment using Multi-Level Spatially Pooled Features

Franz Götz-Hahn, Vlad Hosu, Hanhe Lin, and Dietmar Saupe

Abstract—Video Quality Assessment (VQA) methods have been designed with a focus on particular degradation types, usually artificially induced on a small set of reference videos. Hence, most traditional VQA methods under-perform in-the-wild. Deep learning approaches have had limited success due to the small size and diversity of existing VQA datasets, either artificial or authentically distorted. We introduce a new in-the-wild VQA dataset that is substantially larger and diverse: FlickrVid-150k. It consists of a coarsely annotated set of 153,841 videos having 5 quality ratings each, and 1600 videos with a minimum of 89 ratings each. Additionally, we propose new efficient VQA approaches (MLSP-VQA) relying on multi-level spatially pooled deep features (MLSP). They are extremely well suited for training at scale, compared to deep transfer learning approaches. Our best method MLSP-VQA-FF improves the Spearman Rank-order Correlation Coefficient (SRCC) performance metric on the standard KonVid-1k in-the-wild benchmark dataset to 0.83 surpassing the best existing deep-learning model (0.8 SRCC) and hand-crafted feature-based method (0.78 SRCC). We further investigate how alternative approaches perform under different levels of label noise, and dataset size, showing that MLSP-VQA-FF is the overall best method. Finally, we show that MLSP-VQA-FF trained on FlickrVid-150k sets the new state-of-the-art for cross-test performance on KonVid-1k and LIVE-Qualcomm with a 0.79 and 0.58 SRCC, respectively, showing excellent generalization.

I. INTRODUCTION

VIDEOS have become a central medium for business marketing [1] with over 81% of businesses using video as a marketing tool. Additionally, over 40% of businesses have adopted live video formats such as Facebook Live for marketing and user connection purposes [2]. For consumers, video is the main source of media entertainment, as for example the average US consumer spends 38 hours per week watching video content [3]. It is projected that online videos will make up more than 82% of all consumer internet traffic by 2022 [4], and streaming platforms such as YouTube report that more than a billion hours of video are watched each day [5]. This in part due to consumers believing traditional TV does not offer a good quality of content [3]. Additionally, increased accessibility to video content acquisition hardware, as well as improvements in overall image quality are a central aspect in smartphone technology advancement. Similarly, the rate at which user-generated content is produced is accelerating, but the resulting videos often suffer from quality defects. Therefore it is desirable for a wide range of video producers and consumers to be able to get automated feedback on video quality. For example,

user-generated video distribution platforms like YouTube or Vimeo may want to analyze new videos according to quality to separate professional from amateur video content, instead of only indexing by video playback resolution. Additionally, with an automated Video Quality Assessment (VQA) system, video streaming services can adjust video encoding parameters to maximize video quality.

An important emerging challenge for VQA is to handle in-the-wild videos, which are of arbitrary content and quality representative of internet videos, such as those on YouTube, Flickr, or Vimeo. It comes as no surprise that No-Reference VQA (NR-VQA) in particular has been a field of intensive research in the past few years [6], [7], [8], [9], [10], [11], [12], [13], [14], [15], [16], [17] with large performance improvements. However, state-of-the-art NR-VQA algorithms perform worse on in-the-wild videos than on synthetically distorted ones. These methods aggregate individual video frame quality characteristics that are engineered for specific purposes, such as detecting specific compression artifacts. Often these features trade accuracy for computational efficiency. Furthermore, since there is a lack of large-scale in-the-wild video quality datasets with natural distortions, a thorough evaluation of NR-VQA methods is difficult. Most existing databases are intended as benchmarks for the detection of those specific artificial distortions that NR-VQA algorithms have classically been designed to detect.

To fill this gap our first contribution is the creation of a large ecologically valid dataset, FlickrVid-150k. Similar to Hosu et al. [18], the ecological validity of FlickrVid-150k stems from its size, content diversity, and naturally occurring, and thus representative degradations. However, being two orders of magnitude larger than existing VQA datasets, it poses new challenges to VQA methods, requiring to train across a vast amount of contents and a wide span of authentic distortions. Moreover, since the development of a dataset is usually constrained by a fixed budget, we needed to ensure a minimum level of annotation quality. Therefore, FlickrVid-150k consists in one part of 153,841 five seconds long videos that are annotated by 5 human opinions each (from here on called FlickrVid-150k-A), making it over 125 times larger than existing VQA datasets in terms of number of videos, and with close to one million human ratings over eight times larger in number of annotations [19], [20], [21], [22], [23], [24]. The dataset is accompanied by a benchmark set of nearly 1,600 videos (FlickrVid-150k-B) from the same source with a minimum of 89 opinion scores each. This uniquely opens the possibility of analyzing the trade-off between the amount of training videos and the annotation noise/precision, in terms of

F. Götz-Hahn, V. Hosu, H. Lin and D. Saupe are with the Department of Computer Science, University of Konstanz, 78464 Konstanz, Germany (e-mail: franz.hahn@uni.kn, or firstname.lastname@uni.kn).

the performance on the FlickrVid-150k-B benchmark dataset.

This new dataset aggravates two problems of classical NR-VQA methods. First, the computational costs of hand-crafted feature-based approaches are increased through the sheer number of videos. Second, since hand-crafted features handle in-the-wild videos worse than conventional databases, this dataset is very challenging for classical NR-VQA methods. An alternative to hand-crafted features comes with the rise of deep neural networks (DNNs), where stacked layers of increasingly complex feature detectors are learned directly from observations of input stimuli. These features are often relatively generic, and have been proven to transfer well to similar tasks, that are not too different to the source domain [25], [26]. It is possible to consider a DNN as a feature extractor with a benefit over hand-crafted features in that the features are entirely data-driven.

As a second contribution, we propose to use a new way of extracting video features by aggregating activations of all layers of DNNs pre-trained for classification for a selection of frames. We adopt a strategy similar to Hosu et al. [27] and extract narrow Multi-Level Spatially Pooled (MLSP) features of video frames from an InceptionResNet-v2 [28] architecture to learn VQA. By global average pooling the outputs of inception module activation blocks we obtain fixed sized feature representations of the frames.

The third contribution of this paper consists of two network variants trained on top of the frame feature vectors that surpass state-of-the-art NR-VQA methods and train much faster than the baseline transfer learning approach of fine-tuning the entire source network. We evaluate this approach on existing VQA datasets consisting of natural videos as well as those containing artificially degraded videos and show that on in-the-wild videos the proposed method outperforms classical methods based on hand-crafted features. In particular, training and testing on KonVid-1k improves the state-of-the-art 0.8 to 0.83 SRCC. Finally, we show that training our proposed model on the new dataset of 153,841 videos with five human opinions each achieves 0.79 SRCC in a cross-test on KonVid-1k, outperforming classical approaches that are trained and tested on KonVid-1k (0.78 SRCC), which have the benefit of not being affected by any domain shift [29].

In summary, our main contributions are:

- 1) FlickrVid-150k, an ecologically valid in-the-wild VQA database, two orders of magnitude larger than existing ones
- 2) the successful application of deep MLSP features for VQA
- 3) a DNN model (MLSP-VQA-FF) that surpasses the state-of-the-art with 0.83 SRCC vs the best existing 0.8 SRCC (trained and tested on KonVid-1k); the MLSP-VQA-FF model shows excellent generalization in cross-tests, surpassing the best existing feature-based model that was tested on the same-domain (0.79 on KonVid-1k)

II. RELATED WORK

This paper contributes to both the field of VQA datasets as well as VQA methods. In the following section we will,

therefore, summarize relevant related work in both fields as well as research in the field of feature extraction that was influential in writing this paper.

A. VQA Datasets

There are a few distinguishing factors that separate the field of VQA datasets which are usually governed by decisions made by their creators. We will cover the characteristics which differentiate the broad variety of relevant related works separately.

1) *Video sources*: The first distinguishing factor that heavily influences the use of the dataset is the source of stimuli. The early works in the field of VQA datasets (i.e. EPFL-PoliMI [30], [21], LIVE-VQA [20], [31], CSIQ [19], VQEG-HD [32], and IVP [33]) were mostly concerned with particular compression or transmission distortions. Consequently, early datasets contain few source videos that were degraded to cover the different distortion domains. From today's standpoint the induced degradations lack ecological validity when compared to degradations observed in modern videos in-the-wild. With compression and transmission being largely extraneous factors, due to high quality transmission networks, the focus of VQA datasets has been shifting towards covering a broad diversity of contents and in-the-wild distortions. Recently designed VQA databases (i.e. CVD2014, LIVE-Qualcomm [23], KoNViD-1k [34], and LIVE-VQC [24]) have taken the first steps towards improving ecological validity. CVD2014 contains videos which were degraded with realistic video capture related artifacts. Videos in LIVE-Qualcomm, LIVE-VQC, and KoNViD-1k were either self-recorded or crawled from public domain video sharing platforms without any directed alteration of the content.

An additional side-effect of this change in paradigm are differences in numbers of devices and formats represented in modern datasets. CVD2014 considers videos taken by 78 different cameras with different levels of quality from low-quality camera phones to high-quality digital single lens reflex cameras. The video sequences were captured one at a time from different scenes using different devices. They captured a total of 234 videos (three from each camera) with mixture of in-capture distortions. While each stimulus in CVD2014 is a unique video rather than an alteration of a source video, the dataset only covers five unique scenes, which is the smallest number of unique scenes among all VQA datasets. LIVE-Qualcomm contains videos recorded using eight different mobile cameras at 54 scenes. Dominant frequently occurring distortion types such as insufficient color representation, over/under-exposure, auto-focus related distortions, unsharpness, and stabilization related distortions were introduced during video capturing. In total, the 208 videos cover six types of authentic distortions, but there is no quantification as to how prevalent these distortions are in in-the-wild videos. LIVE-VQC contains videos captured by 80 naïve mobile camera users, totalling 585 unique video scenes at various resolutions and orientations. Finally, KoNViD-1k contains 1,200 unique videos sampled from YFCC100m. It is hard to quantify the number of devices covered, but in terms of content and distortion variety it is the largest existing collection of videos. The videos in KoNViD-1k have been reproduced

from Flickr, based on the highest quality download option, however they are not the raw versions originally uploaded by users. Having been re-encoded to reduce storage requirements, the videos show compression artifacts. We are employing a similar strategy to KoNViD-1k, however we obtain the originally uploaded versions of the videos and re-encode them at a higher quality. We aim to reduce the amount of encoding artifacts, while keeping the file size manageable for use in crowd-sourcing.

2) *Subjective assessment*: The second distinguishing factor is the choice of subjective assessment environment. VQA has been a field of research since before the time where video could easily and reliably be transmitted over the internet. Consequently, early datasets have all been annotated by humans in a lab environment. This allows for assessment of quality under ideal conditions with informed and reliable raters and gives an upper bound to discriminability. With dataset sizes increasing, due to a push for more content diversity, and transmission rates improving, crowdsourcing has become an affordable, and fast way of annotating multimedia datasets with human opinions. The downside is the reduced level of control over the environment and quality of annotation. Careful quality control considerations have to be made to ensure sufficient quality results. Concretely, CVD2014 and LIVE-Qualcomm are annotated in a lab environment, while KoNViD-1k and LIVE-VQC are both annotated using crowdsourcing. Due to the sheer size of our dataset we also resort to crowdsourcing.

3) *Number of observers*: A third factor that has been studied only very little thus far is the choice of numbers of ratings per video. With a few exceptions early works always ensured at least 25 raters per stimulus in the lab environments. Additionally, it has been a common approach that all participants rated all stimuli. Recent works have increased the number of ratings per stimulus to above 200 with the intention of ensuring maximum quality annotation. However, one must consider the trade-off between the benefit of slightly more accurate quality scores from additional ratings for existing stimuli and the potential increase in generalizability of annotation additional stimuli with the same budget. The 8-fold increase in numbers of ratings per stimulus observed when going from the generally accepted 25 to 200 ratings could just as well be an 8-fold increase of numbers of stimuli of 25 ratings. This is especially worth considering in the wake of deep learning approaches outperforming classical methods in a lot of computer vision tasks, as it is known to be robust to noisy labels [35].

Figure 1 shows a comparison of relevant VQA datasets on some of these characteristics. A full list of the distinguishing characteristics of modern databases in comparison to the proposed can be seen in the Appendix in Table VI. There is a progression to a wider variety of contents in the last few years. We are attempting to push this boundary much further, by exploring the trade-off between number of ratings per video and the total annotated stimuli.

B. Feature Extraction

There have been several recent works that inspired our approach for feature extraction. The BLINDER framework

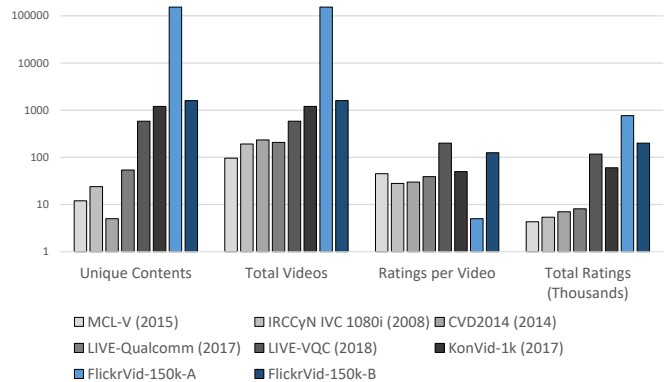


Figure 1. Comparison of characteristics for relevant VQA datasets.

[25] was an initial work that utilized multi-level deep features to predict image quality. They resized images to 224×224 and extracted a feature vector from each layer of a pre-trained VGG-net. Each of these features vectors was then input into separate SVR heads and trained, such that the average layer-wise scores predict the quality of an image. BLINDER was evaluated on a variety of IQA datasets vastly improving the state-of-the-art. Hosu et al. [27] went a step further by utilizing deeper architectures to extract features, such as Inception-v3 and InceptionResNet-v2. Furthermore, they aggregated features from multiple levels, and extracted them from images at their original size. This retained detailed information that would have been lost by down-sizing the inputs. Moreover, it allowed to link information coming from early levels (image dependent) and abstract category-related information from the latter levels in the network.

We use the same approach as presented in [27] to extract features of sets of video frames. The layers of the DNNs are a basic measure for the level of complexity that the feature can represent. First layer features for example resemble Gabor filters or color blobs, while features in higher levels respond to semantic entities such as circular objects with a particular texture or even faces. Changes in the response of different features can therefore encode temporal information. For example it is reasonable to assume that a change in overall response of low-level Gabor-like features can indicate the rapid movement of an object. Consequently, learning from frame-level features allows to indirectly learn the effect of temporal degradations on video quality.

C. NR-VQA

Existing NR-VQA methods can be differentiated on the basis of whether they are based solely on spatial image-level features or also explicitly account for temporal information between sets of frames. In general, however, all recently developed models are learning-based.

Image-based NR-VQA methods are mostly based on theories of human perception, with Natural Scene Statistics (NSS) [36] being the predominant theory used in the Naturalness Image Quality Evaluator (NIQE) [37], Blind/Referenceless Image Spatial Quality Evaluator (BRISQUE) [38], Feature

maps based Referenceless Image Quality Evaluation Engine (FRIQUEE) [39] and High Dynamic Range Image Gradient based Evaluator (HIGRADE) [40]. The theory behind NSS states that certain statistical distributions govern how the human visual system processes particular characteristics of natural images. Image quality can be derived by measuring perturbations of these statistics. The aforementioned approaches have been extended to videos by evaluating them on a representative sample of frames and aggregating them by averaging.

Approaches that consider temporal features, so called general-purpose VQA methods, are less numerous and more particular in their approach. In [9] the authors extended an image-based metric by incorporating time-frequency characteristics and temporal motion information of a given video by means of a motion coherence tensor that summarizes the predominant motion directions over local neighborhoods. The resulting approach, coined V-BLIINDS, has been the de facto standard that new NR-VQA methods are compared with.

Apart from V-BLIINDS, several other machine-learning based models for NR-VQA have been proposed. Regrettably most have only been evaluated on outdated datasets, such as LIVE-VQA, making a comparison difficult, as they are also not publicly available. The three most notable examples are the following. V-CORNIA [39], an unsupervised frame-feature learning approach that uses Support Vector Regression (SVR) to predict frame-level quality. Temporal pooling is then applied to obtain the final video quality. SACONVA [41] extracts feature descriptors using a 3D shearlet transform of multiple frames of a video, which are then passed to a 1D CNN to extract spatio-temporal quality features. COME [42] separated the problem of extracting spatio-temporal quality features into two parts. By fine-tuning AlexNet on the CSIQ dataset, spatial quality features are extracted for each frame by both max pooling and computing the standard deviation of activations in the last layer. Additionally, temporal quality features are extracted as standard deviations of motion vectors in the video. Then, two SVR models are used in conjunction with a Bayes classifier to predict the quality score.

Recently, TLVQM [17] has been proposed. A hierarchical approach for feature extraction, where low complexity features characterizing temporal features of the video are computed for all video frames and high complexity features representing spatial features, such as spatial activity, exposure or sharpness, are extracted from a small representative subset of frames. This approach sets the state-of-the-art for NR-VQA at the time of writing.

III. DATASET IMPLEMENTATION DETAILS

In the following section we will introduce the video dataset in two parts. First, we will discuss the design choices and gathering of the data in Section III-A. Then, Section III-B follows up with details regarding the crowdsourcing experiment to annotate the dataset.

A. Video Dataset

Our main objective was to create a video dataset that covers a broad variety of contents and quality-levels as

commonly available on video sharing websites. For this reason we took a similar approach to collecting our data as the authors of KoNViD-1k with an additional step to improve the quality of the videos. For KoNViD-1k the authors had collected videos which had been transcoded on Flickr, to reduce their storage requirements. Consequently, noticeable degradation was introduced relative to the original uploads. Flickr allows uploading of video files of most codec and container combinations, resolutions, and durations. However, they re-encode the uploaded videos to conventional resolutions (HD, Full HD, etc.), strongly compressing them. The Flickr API allows access to metadata that links to the original, raw uploads. As these raw uploads are often very large, they cannot be used for crowdsourcing. Therefore, we downloaded the authentic raw videos that had an aspect ratio of 16:9 and resolution higher than 960×540 pixels, rescaled them to 960×540 if necessary, cut the middle five seconds, and re-encoded them using FFmpeg at a constant rate factor of 23, which balances visual quality and file size. The resulting files have an average size of 1.23 megabytes. Figure 2 shows an example for visual comparison, where the originally uploaded video is shown in the middle, and our and Flickr’s re-encoded versions are shown to the left and right, respectively. Compression artifacts are clearly visible in the Flickr re-encoded version, whereas our re-encoding is very similar to the original.

For each video we extracted meta-information that identifies the original encoding, including the codec and the bit-rate. Furthermore, we collected social-network attributes such as number of views and likes, and publication date that indicate the popularity of videos. In total, this collection amounts to 153,841 videos. We believe that all the additional measures we have taken to refine our dataset significantly improved its ecological validity, and thus the performance of VQA methods trained on it in the future.

B. Video Annotation

We annotated all 153,783 videos for quality in a crowdsourced setting on Figure Eight¹. First, each participant was presented with instructions according to VQEG recommendations [43], which were modified to our requirements. Here, participants were introduced to the task and provided with information about types of degradation (e.g. poor levels of

¹<http://www.figure-eight.com>

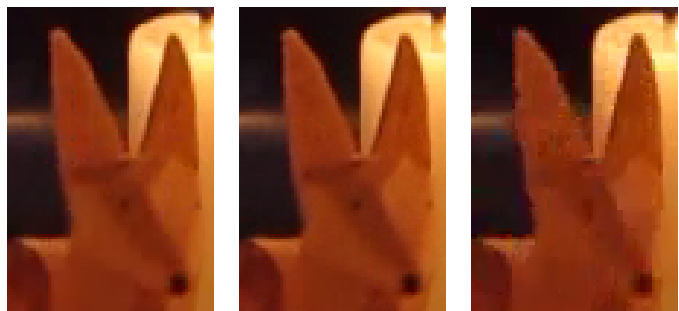


Figure 2. Comparison of the quality of the original (center) to the version Flickr provides (right) and our transcoded version (left).

detail, inconsistencies in color and brightness, or imperfections in motion). Next, we provided examples of videos of a variety of quality levels with a brief description of identifiable flaws, and instructed the reader on the work flow of rating videos, which is illustrated in Figure 3. For each stimulus, workers were first presented with a white box of the size of the video that also functioned as a play button. Then, the video was shown in its place with the playback controls hidden and deactivated. After playback finished it was hidden and the rating scale was revealed below it. This setup ensured that neither the first nor the last still frame of the video were influencing the worker’s rating, and no preemptive rating could be performed, before the entirety of the video had been seen. An option to replay the video was not provided so as to improve attentiveness and ensure that the obtained score is the intuitive response from the worker. Additionally, playback of any other video on the page was disabled until the currently playing video was finished, in order to better control viewing behaviour and discourage unreliable or random answers. Finally, we informed participants about ongoing hidden test questions that were presented throughout the experiment, as well as the minimum resolution requirement that enabled them to continue participating in the experiment. This was checked before the playback of any video.

According to Figure Eight’s design concept crowd workers submit batches of multiple ratings in so called pages. Each page has a fixed batch size of rows, where each row conventionally represents a single item. Due to constraints on the number of rows allowed per study, we grouped 15 stimuli by random selection into each row, with a page size of ten rows per page, totalling to 150 videos per submittable batch. Moreover, the design concept intends a two stage testing process, where workers are first presented with a quiz of test questions followed by subsequent pages where test questions are randomly inserted into the data acquisition process (Illustrated in Figure 4. Test questions are not distinguishable from conventional annotation items. In each row we intersperse three test videos with ground truth with twelve videos randomly sampled from the dataset. The ground truth videos were sampled from hand-picked very high quality videos obtained from Pixabay² or a heavily degraded version of them. We performed a confirmation study to ensure that the perceived quality of these videos were rated at the very top or bottom ends of the 5-point ACR scale. Participants had to retain at least 70% accuracy on test questions throughout the experiment. Data entered from workers that dropped below this threshold was removed and re-entered the pool of data to be annotated.

When running a study on Figure Eight the experimenter decides the number of ratings per data row, as well as the pay per page, which was set, such that with eight seconds per video (five seconds for viewing and three seconds for making the decision) a worker would be paid USD 3 per hour. Based on previous studies we found that a Mean Opinions Score (MOS) made up of 5 ratings has an SRCC of 0.8 with a MOS made up of 50 votes, while two individual MOSes made up of 50 votes have an SRCC of 0.9. Since we have a very large set of

videos we requested 5 individual ratings per data row. However, test rows are not limited to a maximum number of answers. Instead, all crowd workers can technically answer all of the test rows once. Since 12 of the 15 videos in a test row are sampled from the set of data videos we also obtained far more than 5 answers on each of these individual videos. In total, 1,596 data videos were used in test rows and were answered between 89 and 175 times. This very accurately annotated set of videos, called FlickrVid-150k-B, that is ecologically valid and from the same domain as the other data videos will be used as a test set for the evaluation of our models trained on FlickrVid-150k-A.

IV. MODEL IMPLEMENTATION DETAILS

We adopted a similar approach to feature extraction as [27] with their narrow Multi-Level Spatially-Pooled (MLSP) features, but for individual frames of videos, as shown in Fig. 5. In order to extract features we pass individual video frames into an InceptionResNet-v2 network pre-trained on ImageNet[28]. We then perform global average pooling on the activation maps of all kernels in the Stem of the network, as well as in each of the 40 Inception-ResNet modules and the 2 Reduction modules, and concatenate them, resulting in an MLSP feature vector with average activation levels for 16928 kernels of the InceptionResNet-v2 network. For the accurately annotated 1600 videos in FlickrVid-150k-B we extract these MLSP feature vectors for all frames, while for the larger FlickrVid-150k-A we sampled every other frame starting half-way in the video. This choice was primarily driven by the increased storage requirements when saving features from a large number of frames i.e. 392 GB for the features from FlickrVid-150k.

Figure 7 shows a visualization of parts of the MLSP feature vector for multiple consecutive frames.

Different learning-based regression models, such as Support Vector Regression (SVR) or Random Forest Regression (RFR), have been employed to predict subjective quality scores from frame features, with SVR yielding generally better results [17]. However, most existing works only extract a few dozen to a few hundred features. Since SVR is inefficient when applied to very large dimensional features like MLSP and very large numbers of inputs, we instead opt to train two small-capacity DNNs: 1. MLSP-VQA-FF, a feed-forward DNN where the average feature vector is the input of three blocks of fully connected layers with ReLU activations, followed by batch normalization and dropout layers; 2. MLSP-VQA-RN, a deep Long Short-Term Memory (LSTM) architecture, where each LSTM layer receives the feature vector or the hidden state of the lower LSTM layer as an input, and outputs its hidden state. This stacking of layers allows for the simultaneous representation of input series at different time scales [44]. The bottom LSTM layer can be understood as a selective memory of past feature vectors, while each additional LSTM layer represents a selective memory of past hidden states of the previous layer. The final Time Distributed layer preserves a one-to-one relation between input and output, by applying the same operation to the hidden states of the last LSTM layer at all timesteps. The models are depicted in Figure 6. Note that the LSTM network does not

²<http://pixabay.com>



Figure 3. Illustration of the crowdsourcing video playback work flow. A worker is first presented with a white box of 960x540 pixels. Upon clicking the box the video plays in its place. Playback controls are disabled and hidden. Upon finishing the video is hidden and replaced with a white box that informs the participant to rate the quality on the Absolute Category Rating (ACR) scale shown below. The rating scale is also first shown upon completion of video playback.

Table I
TRAINING SETTINGS AND PARAMETERS

| Type | MLSP FF | | | MLSP LSTM | | |
|-----------|---------|------------|-----------|-----------|------------|-----------|
| | frames | batch size | lr | frames | batch size | lr |
| KonVid-1k | all | 128 | 10^{-2} | 180 | 128 | 10^{-4} |
| Qualcomm | all | 8 | 10^{-3} | 150 | 8 | 10^{-4} |
| CVD2014 | all | 8 | 10^{-3} | 140 | 8 | 10^{-4} |
| Proposed | all* | 128 | 10^{-2} | 180 | 128 | 10^{-4} |

utilize dropout of any kind, such as input/output dropout or recurrent dropout, as this resulted in a reduced performance.

The models are trained using the mean square error (MSE) loss for 250 epochs, stopping early if the validation loss did not improve in the most recent 25 epochs at an initial learning rate of 10^{-4} . By default the MLSP-VQA-FF model was trained with a learning rate of 10^{-2} and the MLSP-VQA-RN (LSTM) model was trained with a learning rate of 10^{-4} .

V. MODEL EVALUATION

Our proposed NR-VQA approach of extracting features from a pre-trained classification network and training a DNN architecture on them has been designed with the goal of predicting video quality in-the-wild. We will first evaluate

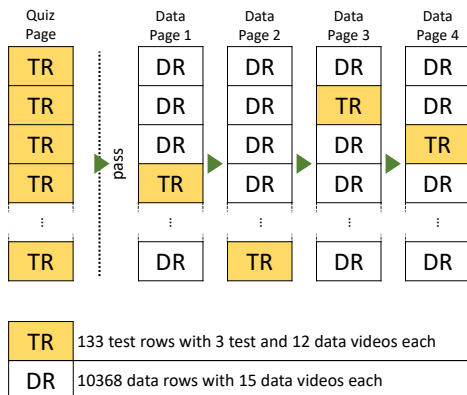


Figure 4. Simplified work flow diagram of the experiment. A worker is first presented with a quiz page of test rows (TR, in yellow) with three test videos and twelve data videos each. Upon passing the quiz with $\geq 70\%$ accuracy they proceed to answer data pages with one test row per page. Data rows (DR, in white) contain 15 data videos. DR are annotated by five unique participants, while unique TR can be answered once by each worker.

the approach by measuring its performance on widely used datasets, namely KoNViD-1k, CVD2014, and LIVE-Qualcomm. There are two fundamental limitations in these datasets that affect the performance of our approach. These relate to the video content, in the form of domain shifts (between ImageNet and the videos), as well as the distributions of subjective video quality ratings (labels).

First, the features in the pre-trained network have been learnt from images in ImageNet. There are situations when the information in the MLSP features may not transfer well to video quality assessment: 1. Some artifacts are unique to video recordings, such is the case of temporal degradations e.g. camera shake, that do not apply to photos. 2. Compression methods are different for videos in comparison to images. Thus, the individual frames may show encoding-specific artifacts that are not within the domain of artifacts present in ImageNet. 3. In-the-wild videos have different types and magnitudes of degradations compared to photos. For example, motion blur degradations can be more prevalent and of a higher magnitude in videos compared to photos. This could affect how well MLSP features from ImageNet transfer to VQA.

Secondly, w.r.t. the subjective video quality ratings to be predicted, while there are similarities between the rating scales used in the subjective studies corresponding to each dataset, the ratings themselves can suffer from a presentation bias. For example, in the case of a dataset with highly similar scenes, but miniscule differences in degradation levels, as is the case for LIVE-Qualcomm and CVD2014, a human observer will become very sensitive to particular degradations. Conversely, the video content becomes less important for quality judgments. The attention of the human observer is diverted to parts in the video he might otherwise not have looked at, had he not seen the same or a very similar scene many times before. Whether the resulting subjective judgments can be regarded as an unbiased quality value is arguable. It is rare that a human observer would watch a scene multiple times before rating the quality. This bias of human opinions will greatly influence how generalizable the quality score is to in-the-wild VQA. Similarly, quality scores obtained in a lab environment will be much more sensitive to differences in technical quality than a worker in a crowdsourcing experiment might be able to pick up. Therefore, it may be challenging to generalize from one experimental setup to another. While consumption of ecologically valid video content happens in a variety of

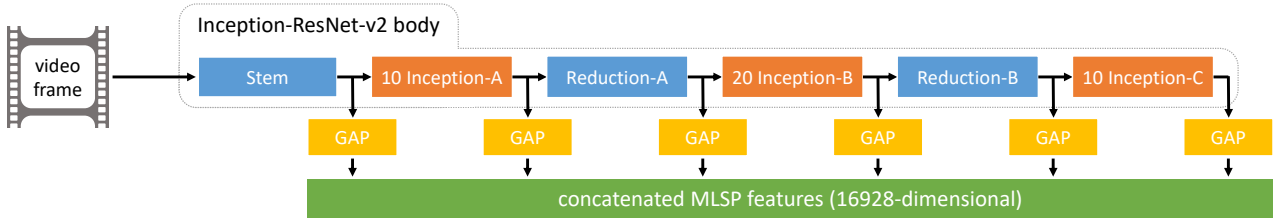


Figure 5. Extraction of Multi-Level Spatially-Pooled (MLSP) features from a video frame, using an InceptionResNet-v2 model pre-trained on ImageNet. The features encode quality-related information: earlier layers describe low-level image details, e.g. image sharpness or noise, and later layers function as object detectors or encode visual appearance information. Global Average Pooling (GAP) is applied to the activations resulting from the Stem, each Inception-module, as well as the Reduction-modules, and finally concatenated to form MLSP features. For more information regarding the individual blocks please refer to the original paper [28].

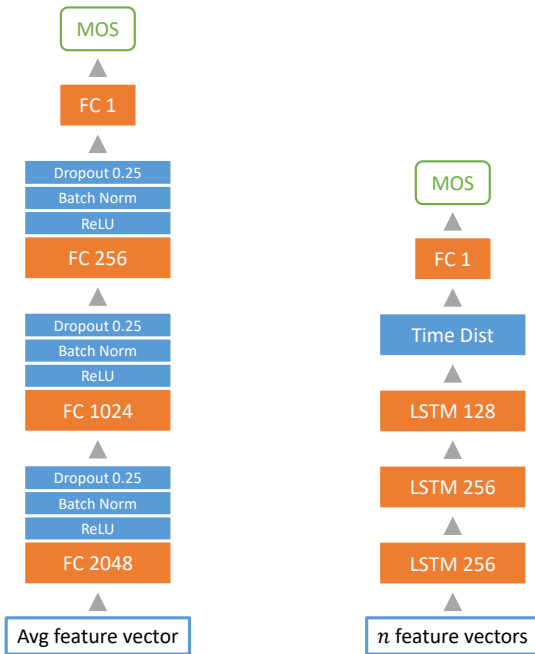


Figure 6. Left: The MLSP-VQA-FF model, that relies on average frame MLSP features and a densely connected Feed Forward network. Right: MLSP-VQA-RN recurrent model, implementing a stacked Long Short-Term Memory network. At each time-step the corresponding frame features are input to the network.

environments and on a multitude of devices, it is arguable whether one experimental setup is superior.

A. Model Performance Comparisons

We first evaluate the performance of the proposed model on three existing authentic video datasets. Each poses a unique challenge for NR-VQA methods. KoNViD-1k is a dataset of natural videos containing distortions that are common to videos hosted on Flickr. LIVE-Qualcomm contains self-recorded scenes of different mobile phone cameras, that were aimed at inducing common distortions. Finally, CVD2014 is a dataset with artificially introduced acquisition-time distortions, however it contains only five unique scenes depicting people. We are comparing our proposed DNN models against other methods which have been thoroughly evaluated on these dataset using

SVR and RFR. Detailed information regarding the experimental evaluation and results of the classical methods can be found in [17]. We adopt a similar testing protocol by training 100 different random splits with 60% of the data used for training, 20% used for validation, and 20% for testing in each split. Table II summarizes the SRCC of all predictions of the classical methods (taken from [17]) alongside our DNN-based approach with the ground-truth, as well as the standard deviations. It is to be noted that the random splits we used are different to the ones used to evaluate the classical methods. For brevity, we are only reporting the results for classical methods obtained using SVR, although three individual results are slightly improved using RFR and are indicated by an asterisk. A complete table for each dataset including the PLCC and RMSE metrics can be found in Appendix .

The FF network outperforms the existing works on KoNViD-1k, improving state-of-the-art SRCC from 0.8 to 0.82, while the LSTM model falls short with an SRCC of 0.79. Nonetheless, this shows that the proposed approaches are competitive on natural videos with some encoding degradations. Since the feature extraction network is trained on images with natural image distortions, it is likely that some of the extracted features are indicative of these distortions, which are not unlike the video encoding artifacts introduced by Flickr.

In the case of LIVE-Qualcomm our best performance of 0.75 SRCC of the LSTM model is surpassed only by TLVQM with 0.78. Since the dataset is comprised of videos containing six different distortion types we also evaluated the performance of the models according to each degradation, as depicted in Figure 8. Here, the deviation for each model is given as a deviation of the RMSE of each distortion type from the average performance in percent. In general, our models perform similarly, with the exception of Color, which the LSTM performs worse on. Videos in the focus degradation class show auto-focus related distortions where parts of the video are intermittently blurry or sharp over time and are overall the biggest challenge for our model. Since this is an artifact that manifests along the temporal dimension it is possible that the LSTM network is able to pick up on these changes in the activations of the frame features and, consequently, performs slightly better. The slight performance gain of the LSTM network on the stabilization distortion category can be argued for in a similar way.

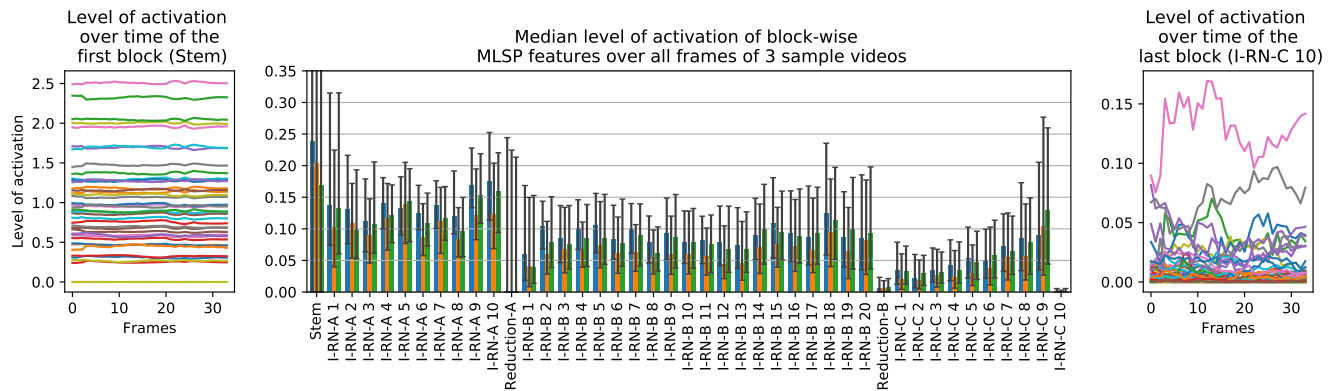


Figure 7. Visualization of the variation of activation levels of MLSP features over the course of FlickrVid-150k videos. In the center the median level of activation for each of the 43 blocks from the Inception-ResNet-v2 network are displayed for 3 sample videos. The black whiskers indicate the 50% confidence interval on the level of activation. For the first block (Stem) the whiskers extend to 0.7. The left and right plots show the activation of 1/8th of the first and last blocks' features over time.

Finally, on CVD2014 our proposed models with SRCCs of 0.77 and 0.71 for the FF and LSTM models, respectively, are outperformed by both FRIQUEE and TLVQM at 0.82 and 0.83 SRCC. CVD2014 is a dataset of videos of two different resolutions, with artificially introduced capturing distortions and only five unique scenes of humans and human faces. The magnitude of the artifacts are at a level that is not commonly seen in videos in-the-wild, and the types of defects is also not within the domain of distortions present in ImageNet. Therefore, this is the most difficult dataset for our approach and, consequently, the relative performance of our approach is worse. CVD2014 is split into six subsets with partially overlapping scenes but distinct capturing cameras. Figure 9 shows the relative deviation of the RMSE from the mean performance for each of these test setups. The first two setups include videos at 640×480 pixels resolution which are generally rated with a lower MOS than videos in the other test setups, which could both be an important factor in our models' increased performance here.

From the previous experiments it is evident that TLVQM is the best performing classical metric on KoNViD-1k. Since FlickrVid-150k-B is quite similar in domain, we compare our MLSP-VQA models against TLVQM as well as V-BLIINDS in Table III. We not only present the results for training and testing on FlickrVid-150k-B, but also denote in the bottom rows the performance when training on the entirety of FlickrVid-150k,

while testing and validating on FlickrVid-150k-B exclusively. Our proposed models outperform the best classical model when trained and tested on the B variant exclusively, although the margin is quite significant with $0.83 > 0.71$. V-BLIINDS improves slightly compared to KoNViD-1k, while TLVQM performs significantly worse overall. Since the main difference between KoNViD-1k and this dataset is the reduced re-encoding degradations, it appears as though the classical methods over-emphasize their prediction on these artifacts.

Additionally, there is a large performance increase when training on FlickrVid-150k-A as well, improving the MLSP-VQA-FF SRCC from 0.72 to 0.80.

B. Evaluation of Training Schemes

With the overall performance of the approach established, we use our two models to explore some open questions regarding training schemes on FlickrVid-150k. As described in Section II-A the choice of numbers of ratings per video is a distinguishing, yet so far unexplored factor in the design of VQA datasets in the context of optimizing model training performance.

As mentioned before, it is common to use an equal number of votes for each stimulus, so that the MOS of the training, validation, and test sets have the same reliability, or level of noise. Deep learning is known to be robust to label noise [35], however this has been only studied when the same amount of

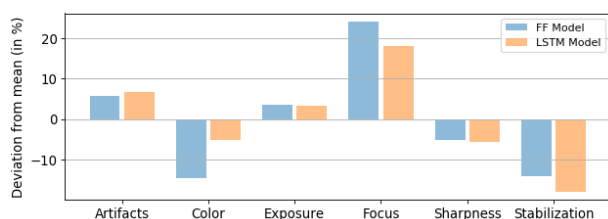


Figure 8. Percent deviation of the mean RMSE of the proposed models on each of the six degradation types present in LIVE-Qualcomm.

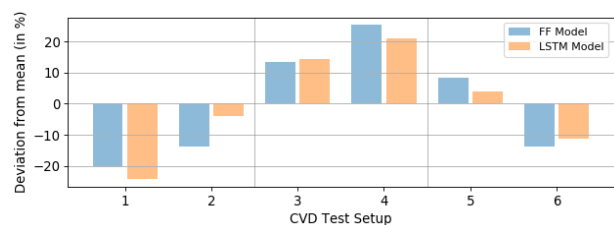


Figure 9. Percent deviation of the mean RMSE of the proposed models on each of the six test scenarios in CVD2014.

Table II
RESULTS OF DIFFERENT NR-VQA METRICS ON DIFFERENT AUTHENTIC VQA DATASETS

| Name | | KoNViD-1k SRCC (\pm STD) | LIVE-Qualcomm SRCC (\pm STD) | CVD2014 SRCC (\pm STD) |
|-----------------|-----------------|-------------------------------------|-------------------------------------|-------------------------------------|
| Classical (SVR) | NIQE (1 fps) | 0.34 (\pm 0.05) | 0.46 (\pm 0.13) | 0.58 (\pm 0.10) |
| | BRISQUE (1 fps) | 0.56 (\pm 0.05) | 0.55 (\pm 0.10) | 0.63 (\pm 0.10) |
| | CORNIA (1 fps) | 0.51 (\pm 0.04) | 0.56 (\pm 0.09) | 0.68 (\pm 0.09) |
| | V-BLIINDS | 0.65 (\pm 0.04) | 0.60 (\pm 0.10) | 0.70 (\pm 0.09) |
| | HIGRADE (1 fps) | 0.73 (\pm 0.03) | 0.68 (\pm 0.08) | 0.74 (\pm 0.06) |
| | FRIQUEE (1 fps) | 0.74 (\pm 0.03) | 0.74 (\pm 0.07) | 0.82 (\pm 0.05) |
| | TLVQM | 0.78 (\pm 0.02) | 0.78 (\pm 0.07) | 0.83 (\pm 0.04) |
| DNN | MLSP-VQA-FF | 0.82 (\pm 0.02) | 0.71 (\pm 0.08) | 0.77 (\pm 0.06) |
| | MLSP-VQA-RN | 0.79 (\pm 0.03) | 0.75 (\pm 0.05) | 0.71 (\pm 0.04) |

Table III
RESULTS OF NR-VQA METRICS ON FLICKRVID-150K-B

| Name | | PLCC (\pm STD) | SRCC (\pm STD) | RMSE (\pm STD) |
|--------------------|-----------------|--------------------|--------------------|----------------------|
| Class. | V-BLIINDS (SVR) | 0.68 (\pm 0.04) | 0.68 (\pm 0.04) | 0.270 (\pm 0.018) |
| | TLVQM (SVR) | 0.68 (\pm 0.12) | 0.71 (\pm 0.04) | 0.263 (\pm 0.040) |
| DNN | MLSP-VQA-FF | 0.72 (\pm 0.12) | 0.69 (\pm 0.13) | 0.478 (\pm 0.381) |
| | MLSP-VQA-RN | 0.77 (\pm 0.10) | 0.75 (\pm 0.10) | 0.298 (\pm 0.035) |
| MLSP-VQA-FF (Full) | | 0.83 (\pm 0.01) | 0.80 (\pm 0.01) | 0.212 (\pm 0.007) |
| MLSP-VQA-RN (Full) | | 0.82 (\pm 0.01) | 0.80 (\pm 0.01) | 0.214 (\pm 0.007) |

noise is present for all items in the dataset (train/test/validation). Thus, the first question we investigate is: *What impact does a different level of noise in the training and validation sets have on test set prediction performance?* More precisely, we are interested to know the change in prediction performance when fewer votes are used for training or validating deep learning models, compared to the number of votes used for test items.

In order to answer this question, we sampled five realizations of the MOS from a set of $v = \{1, 2, 4, 7, 14, 26, 50\}$ votes of FlickrVid-150k-B. We then trained our MLSP-VQA-FF model by varying both training set and validation set MOS vote counts while keeping the test set MOS vote count at 50. For each pair of training and validation MOS we consider twelve random splits with 60% of the data for training, 20% of the data for validation and 20% of the data for testing, with five random initializations each. Therefore, we trained $5 \times 12 \times 7 \times 7 = 2940$ models in total. The graph in Figure 10 depicts the mean SRCC between the models’ predictions and the ground truth MOS of the test sets. Each line in this graph represents a different number of votes comprising the validation MOS, whereas the x-axis indicates the number of votes comprising the training MOS. Please note, that the x-axis is scaled logarithmically for a better visualization. There are three key observations with regard to the prediction performance:

- It improves as the number of votes comprising the training MOS increases, regardless of the number of votes used for validation.
- It improves less beyond 4 votes comprising the training MOS.
- The performance on the test set varies less due to changes in the number of votes used for validation, than it does due to the number of votes for items in the training set.

The fact that performance improves with lower training label

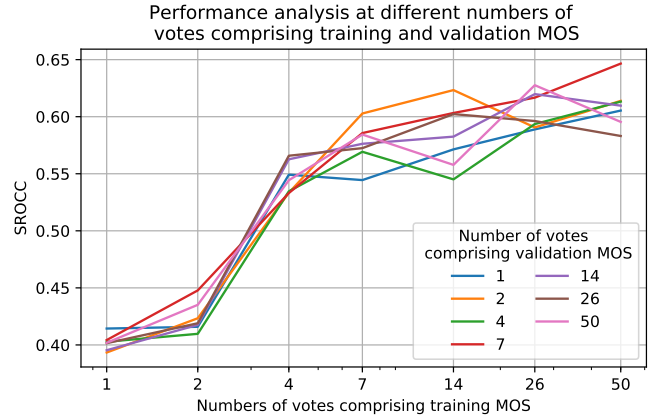


Figure 10. Noise robustness of MLSP feature based method.

noise is not surprising. Nonetheless, the gentler slope for the performance curves beyond 4 votes comprising the training MOS is an indicator that the common policy to gather 25 votes for all stimuli in a dataset is potentially a sub-optimal choice, due to diminishing returns.

The comparison between data splits in this experiment is not entirely fair. All of the points in Figure 10 have different vote budgets. The annotation of a dataset usually has a maximum allocated budget, referring to the total number of judgements that can be collected given a fixed price per judgment. Therefore, the second question we investigate is: *Given a fixed vote budget, how does the allocation of votes on the training set affect test performance?* More precisely, is it better to collect more votes for fewer stimuli, or less votes for

Table IV
TRAINING AT A FIXED VOTE BUDGET OF $\sim 100,000$ VOTES

| | Set | PLCC (\pm STD) | SRCC (\pm STD) | RMSE (\pm STD) |
|------|-------|---------------------|---------------------|-----------------------|
| FF | 1k100 | 0.76 (± 0.03) | 0.73 (± 0.04) | 0.243 (± 0.013) |
| | 20k5 | 0.76 (± 0.02) | 0.74 (± 0.03) | 0.240 (± 0.010) |
| | 100k1 | 0.77 (± 0.02) | 0.74 (± 0.03) | 0.239 (± 0.009) |
| LSTM | 1k100 | 0.77 (± 0.03) | 0.76 (± 0.04) | 0.246 (± 0.020) |
| | 20k5 | 0.79 (± 0.03) | 0.77 (± 0.04) | 0.240 (± 0.017) |
| | 100k1 | 0.78 (± 0.02) | 0.76 (± 0.03) | 0.238 (± 0.010) |

more videos.

In order to answer this question, we first divide FlickrVid-150k-B into five disjoint test sets and sample 25% of the remaining videos of FlickrVid-150k-B for validation, yielding similar sized validation and test sets. We then consider three distributions of $\sim 100,000$ votes across different numbers of videos used for training: 1,000 videos with 100 votes comprising the training MOS (1k100), 20,000 videos with 5 votes comprising the training MOS (20k5), and 100,000 videos with 1 individual vote comprising the training MOS (100k1). For 1k100 we take the remaining 60% of FlickrVid-150k-B (~ 960 videos) as training data. For 20k5 we sample five disjoint sets of $\sim 18,000$ videos from FlickrVid-150k-A and use them alongside the videos in 1k100. Finally, for 100k1 we sample $\sim 95,000$ videos from FlickrVid-150k-A alongside the videos used in 1k100. Since FlickrVid-150k-A is only made up of $\sim 150,000$ videos in total, there is a large overlap between the five training sets for this last experiment.

We train both MLSP-VQA-FF and MLSP-VQA-RN on the five different splits for all three vote budget distributions and report the results in Table IV. We report the PLCC, SRCC as well as RMSE between the model’s predicted scores and the MOS computed by using all available votes. There seems to be very little performance difference between the three sets of vote distributions, with all of them performing within a 0.01 SRCC window for each model. The LSTM network seems to be performing slightly better at 0.76 SRCC, but does not have a significant advantage over the 0.74 SRCC achieved by the FF architecture. The most surprising result is that even with single vote MOSes $\in \{1, \dots, 5\}$, the models are able to make precise predictions. While we cannot conclude based on this experiment which particular vote budget allocation is the best, it is expected that the performance would drop when very few videos are annotated at the same vote budget.

In order to further explore the impact of the vote budget allocation on the generalization performance of our trained models, we evaluated them in cross-tests on KoNViD-1k, LIVE-Qualcomm and CVD2014. The average SRCC performances are reported in Table V. We additionally report cross-test performance using all votes and videos for training using the both MLSP-VQA-FF (*FF Full*) and MLSP-VQA-RN (*LSTM Full*) on FlickrVid-150k. The previous best (*BR*) cross-test performances between the three legacy datasets [17] are reported. Although the performances on the different allocations of our fixed vote budget do not generally vary much, the results reveal some interesting findings.

The cross-test performance on KoNViD-1k of ~ 0.73 SRCC

Table V
CROSS-TEST PERFORMANCE OF MODELS TRAINED USING CONSTANT VOTE BUDGET

| | Set | KoNViD-1k SRCC (\pm STD) | LIVE-Qualcomm SRCC (\pm STD) | CVD2014 SRCC (\pm STD) |
|---------------|-------|-----------------------------|---------------------------------|---------------------------|
| FF | 1k100 | 0.71 (± 0.027) | 0.58 (± 0.032) | 0.46 (± 0.024) |
| | 20k5 | 0.73 (± 0.024) | 0.57 (± 0.058) | 0.48 (± 0.039) |
| | 100k1 | 0.73 (± 0.001) | 0.54 (± 0.009) | 0.41 (± 0.014) |
| LSTM | 1k100 | 0.71 (± 0.023) | 0.58 (± 0.039) | 0.46 (± 0.021) |
| | 20k5 | 0.73 (± 0.025) | 0.58 (± 0.053) | 0.47 (± 0.025) |
| | 100k1 | 0.74 (± 0.004) | 0.59 (± 0.048) | 0.45 (± 0.018) |
| FF | Full | 0.75 (± 0.011) | 0.58 (± 0.017) | 0.54 (± 0.014) |
| LSTM | Full | 0.79 (± 0.008) | 0.51 (± 0.028) | 0.52 (± 0.031) |
| Best Reported | | 0.54 | 0.49 | 0.62 |

is only slightly worse than FRIQUEE (0.74) and TLVQM (0.78), when they are trained and tested on KoNViD-1k directly. Although this dataset does not have the Flickr video encoding artifacts present, it can predict the distorted videos of KoNViD-1k quite well. Furthermore, the cross-test performance on LIVE-Qualcomm of ~ 0.58 average SRCC is roughly around the levels of V-BLIINDS (0.60), when it is trained and tested on LIVE-Qualcomm. Since V-BLIINDS has been the de facto baseline method, it is a noteworthy result. Lastly, the cross-test performance on CVD2014 of ~ 0.46 average SRCC is worse than any existing VQA method trained and tested solely on CVD2014. This may be in part due to the nature of the degradations induced in the creation of the dataset.

When compared to the previously best reported cross-tests, our models have significantly improved performance on KoNViD-1k and LIVE-Qualcomm with $\sim 0.73 > 0.54$ and $\sim 0.58 > 0.49$. However, on CVD2014 our models under-perform compared to the previous best with $\sim 0.46 < 0.62$. Additionally, when using the entire FlickrVid-150k dataset to train, cross-test performances on KoNViD-1k and CVD2014 improves further to 0.75 and 0.54, respectively.

VI. CONCLUSIONS

We introduced a large-scale in-the-wild dataset FlickrVid-150k for video quality assessment (VQA), as well as a novel state-of-the-art no-reference-VQA method for videos in-the-wild. Our learning approach (MLSP-VQA) outperforms the best existing VQA method trained end-to-end, and is substantially faster to train. The large size of the database and efficiency of the learning approach have enabled us to study the effect of different levels of label-noise and how the vote budget affects model performance. We were able to study what happens when keeping the vote budget fixed (total number of collected scores from users), while varying the number of annotated videos. Under a fixed budget, we found that the number of votes allocated to each video is not important for the final model performance when using our MLSP-VQA approach, and other feature-based approaches.

FlickrVid-150k takes a novel approach to VQA, going far beyond the usual in the VQA community. The database is two orders of magnitude larger than previous datasets, it is more authentic both in terms of variety of content types and

distortions, but also due to the compression settings of the videos. We retrieved the original video files uploaded by users from Flickr.com, without the default re-encoding that is generally applied by any video sharing platform to reduce playback bandwidth costs. We encoded the raw video files ourselves at a high enough quality to ensure a good balance between quality and size constraints for crowdsourcing.

The main novelty of the proposed VQA method is frame-level feature extraction using existing DNNs pre-trained for classification, which allows addressing temporal distortions through architectural choices. By global average pooling the activation maps of all kernels in the Inception modules of an InceptionResNet-v2 network trained on ImageNet we extract a wide variety of features, ranging from detections of oriented edges to more abstract ones related to object category. These features are input to two proposed DNN architectures, of which one explicitly makes use of the temporal sequence of the frame features.

We have trained and validated the proposed method on the three most relevant VQA datasets, improving state-of-the-art performance on one of them. While one or two existing works outperform our proposed method on the other two, this is likely due to the artificial nature of degradations in these datasets, that our feature extraction network is not trained on. We also show that our proposed method outperforms the state-of-the-art existing work on FlickrVid-150k-B, the set of 1600 accurately labeled videos that are part of our proposed dataset. Additionally, by training our proposed method on the entirety of the proposed noisily annotated dataset, we are able to improve the cross-test performance on two out of three legacy datasets.

ACKNOWLEDGMENT

Funded by the Deutsche Forschungsgemeinschaft (DFG, German Research Foundation) – Project-ID 251654672 – TRR 161 (Project A05).

REFERENCES

- [1] Wyzowl, “Wyzowl State of Video Marketing Statistics 2019,” <https://info.wyzowl.com/state-of-video-marketing-2019-report>, 2019, [Online; accessed 15-November-2019].
- [2] Buffer, “State Of Social 2019 Report,” <https://buffer.com/state-of-social-2019>, 2019, [Online; accessed 15-November-2019].
- [3] K. Westcott, J. Loucks, K. Downs, and J. Watson, “Digital media trends survey, 12th edition,” 2018.
- [4] V. Cisco, “Cisco visual networking index: Forecast and trends, 2017–2022,” *White Paper*, vol. 1, 2018.
- [5] C. Goodrow, “You know what’s cool? a billion hours,” <https://youtube.googleblog.com/2017/02/you-know-whats-cool-billion-hours.html>, 2017, [Online; accessed 15-November-2019].
- [6] S. Argyropoulos, A. Raake, M.-N. Garcia, and P. List, “No-reference video quality assessment for sd and hd h. 264/avc sequences based on continuous estimates of packet loss visibility,” in *2011 Third International Workshop on Quality of Multimedia Experience*. IEEE, 2011, pp. 31–36.
- [7] Z. Chen and D. Wu, “Prediction of transmission distortion for wireless video communication: Analysis,” *IEEE Transactions on Image Processing*, vol. 21, no. 3, pp. 1123–1137, 2011.
- [8] G. Valenzise, S. Magni, M. Tagliasacchi, and S. Tubaro, “No-reference pixel video quality monitoring of channel-induced distortion,” *IEEE transactions on circuits and systems for video technology*, vol. 22, no. 4, pp. 605–618, 2011.
- [9] M. A. Saad, A. C. Bovik, and C. Charrier, “Blind prediction of natural video quality,” *IEEE Transactions on Image Processing*, vol. 23, no. 3, pp. 1352–1365, 2014.
- [10] K. Pandremmenou, M. Shahid, L. P. Kondi, and B. Lövfström, “A no-reference bitstream-based perceptual model for video quality estimation of videos affected by coding artifacts and packet losses,” in *Human Vision and Electronic Imaging XX*, vol. 9394. International Society for Optics and Photonics, 2015, p. 93941F.
- [11] C. Keimel, J. Habigt, M. Klimpke, and K. Diepold, “Design of no-reference video quality metrics with multiway partial least squares regression,” in *2011 Third International Workshop on Quality of Multimedia Experience*. IEEE, 2011, pp. 49–54.
- [12] K. Zhu, C. Li, V. Asari, and D. Saupe, “No-reference video quality assessment based on artifact measurement and statistical analysis,” *IEEE Transactions on Circuits and Systems for Video Technology*, vol. 25, no. 4, pp. 533–546, 2014.
- [13] J. Sjøgaard, S. Forchhammer, and J. Korhonen, “No-reference video quality assessment using codec analysis,” *IEEE Transactions on Circuits and Systems for Video Technology*, vol. 25, no. 10, pp. 1637–1650, 2015.
- [14] A. Mittal, M. A. Saad, and A. C. Bovik, “A completely blind video integrity oracle,” *IEEE Transactions on Image Processing*, vol. 25, no. 1, pp. 289–300, 2015.
- [15] M. T. Vega, D. C. Mocanu, S. Stavrou, and A. Liotta, “Predictive no-reference assessment of video quality,” *Signal Processing: Image Communication*, vol. 52, pp. 20–32, 2017.
- [16] J. Korhonen, “Learning-based prediction of packet loss artifact visibility in networked video,” in *2018 Tenth International Conference on Quality of Multimedia Experience (QoMEX)*. IEEE, 2018, pp. 1–6.
- [17] J. Korhonen, “Hierarchical approach for no-reference consumer video quality assessment,” 2019.
- [18] V. Hosu, H. Lin, T. Sziranyi, and D. Saupe, “Koniq-10k: An ecologically valid database for deep learning of blind image quality assessment,” 2019.
- [19] E. C. Larson and D. M. Chandler, “Most apparent distortion: full-reference image quality assessment and the role of strategy,” *Journal of Electronic Imaging*, vol. 19, no. 1, p. 011006, 2010.
- [20] K. Seshadrinathan, R. Soundararajan, A. C. Bovik, and L. K. Cormack, “Study of subjective and objective quality assessment of video,” *IEEE transactions on image processing*, vol. 19, no. 6, pp. 1427–1441, 2010.
- [21] F. De Simone, M. Tagliasacchi, M. Naccari, S. Tubaro, and T. Ebrahimi, “A h. 264/avc video database for the evaluation of quality metrics,” in *Acoustics Speech and Signal Processing (ICASSP), 2010 IEEE International Conference on*. IEEE, 2010, pp. 2430–2433.
- [22] M. Nuutinen, T. Virtanen, M. Vaahteranoksa, T. Vuori, P. Oittinen, and J. Häkkinen, “CVD2014— a database for evaluating no-reference video quality assessment algorithms,” *IEEE Transactions on Image Processing*, vol. 25, no. 7, pp. 3073–3086, 2016.
- [23] D. Ghadiyaram, J. Pan, A. C. Bovik, A. K. Moorthy, P. Panda, and K.-C. Yang, “In-capture mobile video distortions: A study of subjective behavior and objective algorithms,” *IEEE Transactions on Circuits and Systems for Video Technology*, 2017.
- [24] Z. Sinno and A. C. Bovik, “Large-scale study of perceptual video quality,” *IEEE Transactions on Image Processing*, vol. 28, no. 2, pp. 612–627, 2019.
- [25] F. Gao, J. Yu, S. Zhu, Q. Huang, and Q. Tian, “Blind image quality prediction by exploiting multi-level deep representations,” *Pattern Recognition*, vol. 81, pp. 432–442, 2018.
- [26] R. Zhang, P. Isola, A. A. Efros, E. Shechtman, and O. Wang, “The unreasonable effectiveness of deep features as a perceptual metric,” in *Proceedings of the IEEE Conference on Computer Vision and Pattern Recognition*, 2018, pp. 586–595.
- [27] V. Hosu, B. Goldlücke, and D. Saupe, “Effective aesthetics prediction with multi-level spatially pooled features,” 2019.
- [28] C. Szegedy, S. Ioffe, V. Vanhoucke, and A. A. Alemi, “Inception-v4, inception-resnet and the impact of residual connections on learning,” in *Thirty-First AAAI Conference on Artificial Intelligence*, 2017.
- [29] S. Ben-David, J. Blitzer, K. Crammer, and F. Pereira, “Analysis of representations for domain adaptation,” in *Advances in neural information processing systems*, 2007, pp. 137–144.
- [30] F. De Simone, M. Naccari, M. Tagliasacchi, F. Dufaux, S. Tubaro, and T. Ebrahimi, “Subjective assessment of h. 264/avc video sequences transmitted over a noisy channel,” in *Quality of Multimedia Experience, 2009. QoMEX 2009. International Workshop on*. IEEE, 2009, pp. 204–209.
- [31] K. Seshadrinathan, R. Soundararajan, A. C. Bovik, and L. K. Cormack, “A subjective study to evaluate video quality assessment algorithms,” in *Human Vision and Electronic Imaging XV*, vol. 7527. International Society for Optics and Photonics, 2010, p. 75270H.

- [32] V. Q. E. Group *et al.*, “Report on the validation of video quality models for high definition video content,” http://www.its.bldrdoc.gov/media/4212/vqeg_hdtv_final_report_version_2.0.zip, 2010.
- [33] F. Zhang, S. Li, L. Ma, Y. C. Wong, and K. N. Ngan, “Ivp subjective quality video database,” *The Chinese University of Hong Kong*, <http://ivp.ee.cuhk.edu.hk/research/database/subjective>, 2011.
- [34] V. Hosu, F. Hahn, M. Jenadeleh, H. Lin, H. Men, T. Szirányi, S. Li, and D. Saupe, “The Konstanz Natural Video Database KoNViD-1k,” in *9th Int. Conf. on Quality of Multimedia Experience (QoMEX)*, 2017.
- [35] D. Rolnick, A. Veit, S. Belongie, and N. Shavit, “Deep learning is robust to massive label noise,” *arXiv preprint arXiv:1705.10694*, 2017.
- [36] A. Srivastava, A. B. Lee, E. P. Simoncelli, and S.-C. Zhu, “On advances in statistical modeling of natural images,” *Journal of Mathematical Imaging and Vision*, vol. 18, no. 1, pp. 17–33, 2003.
- [37] A. Mittal, R. Soundararajan, and A. C. Bovik, “Making a “completely blind” image quality analyzer,” *IEEE Signal Processing Letters*, vol. 20, no. 3, pp. 209–212, 2012.
- [38] A. Mittal, A. K. Moorthy, and A. C. Bovik, “No-reference image quality assessment in the spatial domain,” *IEEE Transactions on image processing*, vol. 21, no. 12, pp. 4695–4708, 2012.
- [39] J. Xu, P. Ye, Y. Liu, and D. Doermann, “No-reference video quality assessment via feature learning,” in *2014 IEEE international conference on image processing (ICIP)*. IEEE, 2014, pp. 491–495.
- [40] D. Kundu, D. Ghadiyaram, A. C. Bovik, and B. L. Evans, “No-reference quality assessment of tone-mapped hdr pictures,” *IEEE Transactions on Image Processing*, vol. 26, no. 6, pp. 2957–2971, 2017.
- [41] Y. Li, L.-M. Po, C.-H. Cheung, X. Xu, L. Feng, F. Yuan, and K.-W. Cheung, “No-reference video quality assessment with 3d shearlet transform and convolutional neural networks,” *IEEE Trans. Circuits Syst. Video Techn.*, vol. 26, no. 6, pp. 1044–1057, 2016.
- [42] C. Wang, L. Su, and W. Zhang, “Come for no-reference video quality assessment,” in *2018 IEEE Conference on Multimedia Information Processing and Retrieval (MIPR)*. IEEE, 2018, pp. 232–237.
- [43] ITU-T, “Objective perceptual assessment of video quality: Full reference television,” Tutorial, ITU-T Telecommunication Standardization Bureau, 2004.
- [44] M. Hermans and B. Schrauwen, “Training and analysing deep recurrent neural networks,” in *Advances in neural information processing systems*, 2013, pp. 190–198.

APPENDIX A

Table VI
ATTRIBUTES OF EXISTING VQA DATABASES. OUR PROPOSED DATABASES (KONVID-150K, KONVID-1600) ARE DISPLAYED IN BOLD.

| Attribute / Database | CVD2014 | LIVE-Q. | KoNViD-1k | LIVE-VQC | FlickrVid-150k-A | FlickrVid-150k-A |
|----------------------|----------|---------|-----------|----------|------------------|------------------|
| Year | 2016 | 2017 | 2017 | 2019 | 2019 | 2019 |
| Unique contents | 5 | 54 | ≈ 1200 | ≈ 585 | ≈ 150,000 | 1600 |
| Stimuli | 234 | 208 | 1200 | 585 | 153,841 | 1600 |
| Ratings per Video | 27-33 | 39 | 50 | >200 | 5 | 89-175 |
| Devices | 78 | 8 | N/A | 43 | ≈ 4500(?)* | (?) |
| Duration | 10-25 | 15 | 8 | 10 | 5 | 5 |
| Resolution | VGA/720p | 1080p | 540p | various | 540p | 540p |
| Frame Rate | 10-31 | 30 | 30 | N/A | 24-120 | 24-120 |
| Format | various | YUV | MPEG-4 | N/A | MPEG-4 | MPEG-4 |

Table VII
RESULTS OF NR-VQA METRICS ON KONVID-1K

| | Name | PLCC (± STD) | SRCC (± STD) | RMSE (± STD) |
|-----------|----------------------|----------------------|----------------------|------------------------|
| Classical | NIQE (1 fps, SVR) | 0.34 (± 0.05) | 0.34 (± 0.05) | 0.606 (± 0.026) |
| | BRISQUE (1 fps, RFR) | 0.58 (± 0.04) | 0.58 (± 0.04) | 0.518 (± 0.022) |
| | CORNIA (1 fps, SVR) | 0.51 (± 0.04) | 0.51 (± 0.04) | 0.560 (± 0.024) |
| | V-BLIINDS (RFR) | 0.64 (± 0.04) | 0.65 (± 0.04) | 0.490 (± 0.022) |
| | HIGRADE (1 fps, SVR) | 0.72 (± 0.03) | 0.73 (± 0.03) | 0.444 (± 0.023) |
| | FRIQUEE (1 fps, SVR) | 0.74 (± 0.03) | 0.74 (± 0.03) | 0.432 (± 0.022) |
| | TLVQM (SVR) | 0.77 (± 0.02) | 0.78 (± 0.02) | 0.406 (± 0.018) |
| DNN | Proposed FF | 0.83 (± 0.02) | 0.82 (± 0.02) | 0.370 (± 0.019) |
| | Proposed LSTM | 0.80 (± 0.03) | 0.79 (± 0.03) | 0.402 (± 0.030) |

Table VIII
RESULTS OF NR-VQA METRICS ON LIVE-QUALCOMM

| | Name | PLCC (± STD) | SRCC (± STD) | RMSE (± STD) |
|-----------|----------------------|----------------------|----------------------|--------------------|
| Classical | NIQE (1 fps, SVR) | 0.48 (± 0.12) | 0.46 (± 0.13) | 10.7 (± 1.3) |
| | BRISQUE (1 fps, SVR) | 0.54 (± 0.10) | 0.55 (± 0.10) | 10.3 (± 0.9) |
| | CORNIA (1 fps, SVR) | 0.61 (± 0.09) | 0.56 (± 0.09) | 9.7 (± 0.9) |
| | V-BLIINDS (SVR) | 0.67 (± 0.09) | 0.60 (± 0.10) | 9.2 (± 1.0) |
| | HIGRADE (1 fps, SVR) | 0.71 (± 0.08) | 0.68 (± 0.08) | 8.6 (± 1.1) |
| | FRIQUEE (1 fps, SVR) | 0.78 (± 0.06) | 0.74 (± 0.07) | 7.6 (± 0.8) |
| | TLVQM (SVR) | 0.81 (± 0.06) | 0.78 (± 0.07) | 7.1 (± 1.0) |
| DNN | Proposed FF | 0.73 (± 0.07) | 0.71 (± 0.08) | 8.4 (± 1.0) |
| | Proposed LSTM | 0.76 (± 0.06) | 0.75 (± 0.05) | 8.2 (± 1.0) |

Table IX
RESULTS OF NR-VQA METRICS ON CVD2014

| | Name | PLCC (± STD) | SRCC (± STD) | RMSE (± STD) |
|-----------|----------------------|----------------------|----------------------|---------------------|
| Classical | NIQE (1 fps, SVR) | 0.61 (± 0.09) | 0.58 (± 0.10) | 17.1 (± 1.5) |
| | BRISQUE (1 fps, RFR) | 0.67 (± 0.09) | 0.65 (± 0.10) | 15.9 (± 1.8) |
| | CORNIA (1 fps, SVR) | 0.71 (± 0.08) | 0.68 (± 0.09) | 15.2 (± 1.6) |
| | V-BLIINDS (RFR) | 0.74 (± 0.07) | 0.73 (± 0.08) | 14.6 (± 1.6) |
| | HIGRADE (1 fps, SVR) | 0.76 (± 0.06) | 0.74 (± 0.06) | 14.2 (± 1.5) |
| | FRIQUEE (1 fps, SVR) | 0.83 (± 0.04) | 0.82 (± 0.05) | 12.0 (± 1.2) |
| | TLVQM (SVR) | 0.85 (± 0.04) | 0.83 (± 0.04) | 11.3 (± 1.3) |
| DNN | Proposed FF | 0.78 (± 0.05) | 0.77 (± 0.06) | 13.5 (± 1.5) |
| | Proposed LSTM | 0.75 (± 0.04) | 0.71 (± 0.04) | 13.9 (± 0.6) |